A Simple Model of Current Ramp-Up and Ramp-Down in Tokamaks

Richard Fitzpatrick [a]

Institute for Fusion Studies, Department of Physics,

University of Texas at Austin, Austin TX 78712

----

[a] rfitzp@utexas.edu

I. INTRODUCTION

In a recent paper, Boozer[1] argues that Faraday's law of electric induction places strong constraints on the operation of a future tokamak fusion power plant. In particular, Boozer takes issue with the claim by de Vries et alia[2] that a fully controlled current ramp-down in the future ITER tokamak, starting from a toroidal plasma current of 15 MA, can be effected in 60 seconds. (Indeed, in an earlier study Boozer[3] seems to argue that the true ramp time is 1000 seconds.) Boozer also takes issue with the claim by Creely et alia[4] that the plasma current in the future SPARC tokamak can be ramped up in 7 seconds, and ramped down in 12 seconds, and seems to imply that the true ramp time, in fact, 1157 seconds. The claim by de Vries et alia is made in Sect. 2 of Ref. 2, and is based on simulations performed using the CORSICA[5,6] code. The claim by Creely et alia is deduced from in Fig. 3 of Ref. 4, and is based on simulations made with the TSC[7] code. While it is the case that the CORSICA and TSC codes both have a proven track records, we can certainly agree with Boozer that neither de Vries et alia or Creely et alia provide sufficient information to validate their claims. To help clarify the situation, this paper presents a simple model of current ramp-up and ramp-down in tokamak plasmas. The aim of the paper is to determine, in a transparent manner, whether the claims by de Vries et alia and Creely et alia are, at least, plausible, and also to clarify the constraints that Faraday's law actually do place on future tokamak operation. Boozer[1,3] also highlights the danger of runaway electron generation during current ramps, so we shall also try to estimate the likelihood of dangerous levels of runaway electron generation during current ramps in future tokamaks.

II. TOKAMAK OPERATION

Figure 1 is a cartoon that illustrates how a current ramp-up is effected in a conventional tokamak plasma.[8–11] After the initial burn-through phase, the fully ionized plasma starts off as an ohmic discharge of circular poloidal cross-section, and relatively small minor radius, that is limited on the first wall, and carries a comparatively small toroidal current. As the toroidal current is gradually increased, the minor radius and vertical elongation of the

plasma increase in concert, but the plasma remains limited on the first wall. (See Fig. 7 of Ref. 8 and Fig. 1 of Ref. 9.) Only in the very final stages of the current ramp is the magnetic X-point added to the equilibrium, at which point the plasma becomes diverted, and consequently ceases to be limited by the first wall.

The current ramp usually takes place in two stages. In the first stage, the edge safety-factor, q_a, of the plasma is allowed to decrease from an initially very large value to its final value of about 3.5, at fixed plasma minor radius. In the second stage, which is usually much longer than the first, q_a is held constant while the plasma expands in volume. The first stage is hazardous because, as q_a passes through integer values (6, 5, 4, et cetera), the plasma becomes momentarily susceptible to both tearing and ideal-kink modes.[12,13] However, the degree of the hazard is mitigated by the smallness of the plasma current. In the second stage, the safety-factor profile is held approximately constant, and is designed to be stable to both tearing and ideal-kink modes.

After the current ramp has been completed, and the magnetic diverter is operational, external heating is applied to the plasma discharge, while the current is held constant. Consequently, the plasma eventually attains its peak temperature. The current flat-top phase of the plasma discharge is usually much longer in duration than both the current ramp-up and ramp-down phases. Toward the end of the current flat-top, the external heating is turned off, and the plasma eventually returns to the same state that it was in at the end of the current ramp-up. At this stage, the sequence of events that constitute the current ramp-up is carried out in reverse order to effect a current ramp-down. In other words, the magnetic X-point is first removed from the plasma, which then becomes limited by the first wall. The plasma is then gradually crushed against the first wall, while the current is reduced, but q_a is held constant. (See Fig. 7 of Ref. 8.) Finally, q_a is allowed to rise to a large value, at fixed minor radius, as last remnants of the plasma current disappear.

3

III.   ANALYSIS

A.   Coordinates

Let us model a tokamak plasma, in the simplest imaginable manner, as a periodic cylinder. Let r, θ, z be conventional cylindrical coordinates, and let the magnetic axis of the plasma correspond to $r = 0$. The system is assumed to be periodic in z with period length $2\pi\,R_0$, where R_0 is the simulated major radius of the plasma. Let a be the minor radius of the plasma at the end of the current ramp.

B.   Fundamental Equations

The equilibrium magnetic field is represented as

$$\mathbf{B}(r,t) = B_\theta(r,t)\,\mathbf{e}_\theta + B_0\,\mathbf{e}_z, \tag{1}$$

where B_0 is the constant toroidal magnetic field generated by currents flowing in external field-coils. The poloidal field, $B_\theta(r,t)$, on the other hand, is generated via transformer action. The current density in the plasma is written $\mathbf{j} = j_z\,\mathbf{e}_z$. Moreover, Ampère's law implies that

$$\mu_0\,j_z(r,t) = \frac{1}{r}\frac{\partial}{\partial r}(r\,B_\theta). \tag{2}$$

The total toroidal current carried by the plasma is

$$I_p(t) = \kappa \int_0^a 2\pi\,r\,j_z\,dr = \frac{2\pi\,\kappa\,a\,B_\theta(a,t)}{\mu_0}. \tag{3}$$

Here, we have crudely taken into account the vertical elongation, κ, of the plasma, which leads to an increases in the plasma poloidal cross-section. The plasma safety-factor profile takes the form

$$q(r,t) = \frac{r\,B_0}{R_0\,B_\theta}, \tag{4}$$

while the electric field in the plasma is written $\mathbf{E} = E_z\,\mathbf{e}_z$. Faraday's law yields

$$\frac{\partial E_z}{\partial r} = \frac{\partial B_\theta}{\partial t}. \tag{5}$$

4

Ohm's law gives

$$E_z = \eta\, j_z, \tag{6}$$

where

$$\eta = \frac{Z \ln \Lambda}{1.96\, 6\sqrt{2}\, \pi^{3/2}}\, \frac{m_e^{1/2}\, e^{2}\, c^{4}\, \mu_0^2}{T_e^{3/2}} \tag{7}$$

is the Spitzer resistivity.[14,15] Here, $T_e(r,t)$ is the electron temperature profile, Z the effective ion charge number, $\ln \Lambda \simeq 15$ the Coulomb logarithm, m_e the electron mass, e the magnitude of the electron charge, c the velocity of light in vacuum, and μ_0 the vacuum permeability. Note that, for the sake of simplicity, we are neglecting both the neoclassical increase in the plasma resistivity, as well as the non-inductive bootstrap current.[16] Finally, it is helpful to define the poloidal magnetic flux, $\psi(r,t)$, where

$$B_\theta = \frac{1}{2\pi\, R_0}\, \frac{\partial \psi}{\partial r}. \tag{8}$$

The electron energy balance equation takes the form [15]

$$\frac{3}{2}\, n_e\, \frac{\partial T_e}{\partial t} - n_e\, \frac{1}{r}\, \frac{\partial}{\partial r} \left(r\, \chi_\perp\, \frac{\partial T_e}{\partial r} \right) = \eta\, j_z^2, \tag{9}$$

where n_e is the electron number density, and $\chi_\perp(r)$ is the electron perpendicular energy diffusivity due to small-scale plasma turbulence. Note that, for the sake of simplicity, we are treating n_e as a spatial and temporal constant. Moreover, we expect $\chi_\perp \sim 1\, \mathrm{m^2\, s^{-1}}$.[17] Finally, the net power input to the plasma due to ohmic heating is

$$P(t) = 4\pi^2\, \kappa\, R_0 \int_0^a r\, \eta\, j_z^2\, dr, \tag{10}$$

where we have again crudely allowed for the plasma elongation.

C. Fundamental Quantities

Let $\epsilon = a/R_0$ be the inverse aspect-ratio of the plasma, q_a the value of the edge safety-factor at the end of the current ramp, and

$$B_{\theta\, a} = \frac{\epsilon}{q_a}\, B_0 \tag{11}$$

the edge poloidal magnetic field at the end of the current ramp. Suppose that $\chi_{\perp}(r) = \chi_0\,\hat{\chi}(r)$, where χ_0 is a typical value of the perpendicular energy diffusivity, and $\hat{\chi}(r)$ is dimensionless and of order unity. We can define

$$T_0 = \left[\frac{Z\,\ln\Lambda}{1.96\,6\sqrt{2}\,\pi^{3/2}}\,\frac{m_e^{1/2}\,e^2\,c^4\,B_{\theta\,a}^2}{n_e\,\chi_0}\right]^{2/5} \tag{12}$$

$$= 9.95\times10^{-1}\,Z^{2/5}\,\Lambda_{15}^{2/5}\,n_{20}^{-2/5}\,\chi_0^{-2/5}\,B_{\theta\,a}^{4/5}\ \mathrm{keV} \tag{13}$$

as the typical electron temperature attained at the end of the current ramp. Here, $\Lambda_{15} = \ln\Lambda/15$ and $n_{20} = n_e/10^{20}$. All other quantities are in SI units. Likewise,

$$\tau_R \equiv \frac{a^2\,\mu_0}{\eta(T_0)} = 4.99\times10^1\,a^2\,Z^{-2/5}\,\Lambda_{15}^{-2/5}\,n_{20}^{-3/5}\,\chi_0^{-3/5}\,B_{\theta\,a}^{6/5}\ \mathrm{s} \tag{14}$$

is the conventional resistive diffusion time, whereas

$$\tau_c = \frac{a^2}{\chi_0}\ \mathrm{s} \tag{15}$$

is the energy confinement time. The plasma poloidal beta is defined

$$\beta_p \equiv \frac{\mu_0\,n_e\,T_0}{B_{\theta\,a}^2} = 2.00\times10^{-2}\,Z^{2/5}\,\Lambda_{15}^{2/5}\,n_{20}^{3/5}\,\chi_0^{-2/5}\,B_{\theta\,a}^{-6/5}. \tag{16}$$

Note that

$$\beta_p = \frac{\tau_c}{\tau_R} \tag{17}$$

in an ohmic plasma. The typical plasma current is

$$I_0 = \frac{2\pi\,\kappa\,a\,B_{\theta\,a}}{\mu_0} = 5.00\,\kappa\,a\,B_{\theta\,a}\ \mathrm{MA}. \tag{18}$$

The typical electric field-strength in the plasma takes the form

$$E_0 = \frac{\beta_p\,\chi_0\,B_{\theta\,a}}{a} = 2.00\times10^{-2}\,a^{-1}\,Z^{2/5}\,\Lambda_{15}^{2/5}\,n_{20}^{3/5}\,\chi_0^{3/5}\,B_{\theta\,a}^{-1/5}\ \mathrm{V\,m^{-1}}. \tag{19}$$

The typical ohmic heating power is

$$P_0 = 4\pi^2\,\kappa\,R_0\,n_e\,\chi_0\,T_0 = 6.29\times10^{-1}\,\kappa\,R_0\,Z^{2/5}\,\Lambda_{15}^{2/5}\,n_{20}^{3/5}\,\chi_0^{3/5}\,B_{\theta\,a}^{4/5}\ \mathrm{MW}. \tag{20}$$

Finally, the typical poloidal flux takes the form

$$\psi_0 = 6.28\,R_0\,a\,B_{\theta\,a}\ \mathrm{V\,s}. \tag{21}$$

D. Runaway Electron Generation

The plasma at the start of the current ramp is cold and resistive. Consequently, driving a current through the discharge requires a comparatively large inductive electric field. In such circumstances, there is a danger of runaway electron generation. Runaway electrons are suprarthermal electrons for which the Coulomb collisional drag due to the bulk plasma is less than the acceleration due to the inductive electric field. Such electrons can acquire energies in excess of 10 MeV, and cause considerable damage if they strike the first wall.

Runaway electron generation is only possible, in theory, when the electric field exceeds the so-called *Connor-Hastie* value,[18]

$$E_c = \frac{\ln \Lambda \, n_e \, e^3}{4\pi \, \epsilon_0^2 \, m_e \, c^2} = 7.65 \times 10^{-2} \, \Lambda_{15} \, n_{20} \ \mathrm{V\,m^{-1}}. \tag{22}$$

Here, ϵ_0 is the vacuum permittivity. However, the criterion $E > E_c$ does not, by itself, guarantee the generation of dangerous quantities of runaway electrons, because, before this can happen, there needs to be a source of suprathermal electrons. On obvious source is from the high-energy tail of the thermal electrons. However, it is well-known that this source does not become effective until the electric field approaches the so-called *Driecer* value,[19]

$$E_D = E_c \, \frac{m_e \, c^2}{T_e} = E_{D0} \, \frac{T_e}{T_0}, \tag{23}$$

where

$$E_{D0} = 3.93 \times 10^1 \, Z^{-2/5} \, \Lambda_{15}^{3/5} \, n_{20}^{7/5} \, \chi_0^{2/5} \, B_{\theta \, a}^{-4/5} \ \mathrm{V\,m^{-1}}. \tag{24}$$

Note that $E_{D0} \gg E_c$.

In an extensive study of runaway electron generation in the JET tokamak,[20] de Vries et alia find that JET plasmas invariably satisfy the runaway electron existence criterion, $E > E_c$, in the early stages of the discharge, but that this does not usually lead to the generation of dangerous quantities of runaway electrons. In fact, de Vries et alia conclude that $E > 10 \, E_c$ is needed before runaway electron generation becomes a problem. This conclusion is consistent with those of earlier studies.[21-23]

E. Normalization

Let us adopt the following convenient normalization scheme: $r = a\,\hat{r}$, $t = \tau_R\,\hat{t}$, $T_e = T_0\,\hat{T}(\hat{r}, \hat{t})$, $B_\theta = B_{\theta\,a}\,\hat{B}_\theta(\hat{r}, \hat{t})$, $I_p = I_0\,\hat{I}_p(\hat{t})$, $j_z = [B_{\theta\,a}/(\mu_0\,a)]\,\hat{j}$, $E = E_0\,\hat{E}(\hat{r}, \hat{t})$, $E_c = E_0\,\hat{E}_c$, $E_D = E_0\,\hat{E}_D(\hat{r}, \hat{t})$, $E_{D\,0} = E_0\,\hat{E}_{D\,0}$, $P = P_0\,\hat{P}(\hat{t})$, and $\psi = \psi_0\,\hat{\psi}(\hat{r}, \hat{t})$. It follows that

$$\frac{3}{2}\,\beta_p\,\frac{\partial \hat{T}}{\partial \hat{t}} = \frac{\partial^2 \hat{T}}{\partial \hat{r}^2} + \frac{1}{\hat{r}}\,\frac{\partial \hat{T}}{\partial \hat{r}} + \frac{d\ln\hat{\chi}}{d\hat{r}}\,\frac{\partial \hat{T}}{\partial \hat{r}} + \frac{\hat{E}^2\,\hat{T}^{3/2}}{\hat{\chi}}, \tag{25}$$

$$\frac{\partial \hat{B}_\theta}{\partial \hat{r}} + \frac{\hat{B}_\theta}{\hat{r}} = \hat{E}\,\hat{T}^{3/2}, \tag{26}$$

$$\frac{\partial \hat{B}_\theta}{\partial \hat{t}} = \frac{\partial \hat{E}}{\partial \hat{r}}, \tag{27}$$

as well as

$$\frac{q}{q_a} = \frac{\hat{r}}{\hat{B}_\theta}, \tag{28}$$

$$\hat{I}_p(\hat{r}, \hat{t}) = \hat{r}\,\hat{B}_\theta(\hat{r}, \hat{t}), \tag{29}$$

$$\hat{B}_\theta = \frac{\partial \hat{\psi}}{\partial \hat{r}}, \tag{30}$$

$$\hat{E}_D = \hat{E}_{D\,0}\,\hat{T}^{-1}, \tag{31}$$

Here, $\hat{I}_p(\hat{r}, \hat{t})$ is the toroidal plasma current contained within normalized minor radius $\hat{r}$. Equations (27) can be integrated to give

$$\hat{E}(\hat{r}, \hat{t}) = \frac{\partial \hat{\psi}}{\partial \hat{t}} = \mathcal{E}(\hat{t}) + \int_0^{\hat{r}} \frac{\partial \hat{B}_\theta}{\partial \hat{t}}\,d\hat{r}', \tag{32}$$

where use has been made of Eq. (30). It follows that

$$\mathcal{E}(\hat{t}) = \frac{\partial \hat{\psi}(0, \hat{t})}{\partial \hat{t}}. \tag{33}$$

Finally, it can be shown that

$$\hat{E}_c = 3.82\,a\,Z^{-2/5}\,\Lambda_{15}^{3/5}\,n_{20}^{2/5}\,\chi_0^{-3/5}\,B_{\theta\,a}^{1/5}, \tag{34}$$

$$\hat{E}_{D\,0} = 1.96 \times 10^3\,Z^{-4/5}\,\Lambda_{15}^{3/5}\,n_{20}^{4/5}\,\chi_0^{-1/5}\,B_{\theta\,a}^{-3/5}. \tag{35}$$

F. Approximations

In order to facilitate our analysis, we make two approximations. Our first approximation is to neglect the term involving β_p in Eq. (25). This approximation is warranted because, as is clear from Eq. (16), β_p is much less than unity in conventional ohmic tokamak plasmas. As is apparent from Eq. (17), this is the case because the energy confinement time is much less than the resistive diffusion time in such plasmas. The neglect of the term in question implies that, during the current ramp, the temperature profile remains in a quasi-equilibrium state in which the energy per unit time that flows across the plasma boundary, and is presumably absorbed by the limiter, matches the ohmic heating power. Under these circumstances, the normalized ohmic heating power is written

$$\hat{P}(\hat{t}) = -\left(\hat{\chi}\,\hat{r}\,\frac{\partial \hat{T}}{\partial \hat{r}} \right)_{\hat{r}=1}. \tag{36}$$

Our second approximation is to neglect the second term on the extreme right-hand side of Eq. (32). The neglect of the term in question implies that the inductive electric field is uniform within the plasma. Of course, this is the usual situation during the current flat-top phase of a tokamak discharge. However, it is possible for the electric field to be spatially constant during a current ramp as long as the current is not ramped up or down too rapidly. Indeed, the criterion that must be satisfied is

$$\mathcal{E} > \left| \int_0^1 \frac{\partial \hat{B}_\theta}{\partial \hat{t}}\,d\hat{r}' \right|. \tag{37}$$

During the ramp-up phase, if the current is ramped up sufficiently rapidly that the criterion (37) is not satisfied then the electric field in the outer regions of the plasma becomes greater than that in the core, leading to a broadening of the current profile. However, a broad current profile implies a low internal plasma inductance, and low-inductance plasmas are prone to destructive ideal-kink instabilities.[12,13] During the ramp-down phase, on the other hand, if the current is ramped down sufficiently rapidly that the criterion (37) is not satisfied then the electric field in the outer regions of the plasma becomes less than that in the core, leading to a peaking of the current profile. However, plasmas with strongly peaked current profiles are prone to tearing instabilities that can lead to disruptions.[12,13]

Thus, the criterion (37) is a necessary one for the safe operation of a tokamak during the current ramp-up and ramp-down phases.

Our two approximations lead to the following equations:

$$\frac{\partial^2 \hat{T}}{\partial \hat{r}^2} + \frac{1}{\hat{r}} \frac{\partial \hat{T}}{\partial \hat{r}} + \frac{d \ln \hat{\chi}}{d \hat{r}} \frac{\partial \hat{T}}{\partial \hat{r}} + \frac{\mathcal{E}^2 \hat{T}^{3/2}}{\hat{\chi}} = 0, \tag{38}$$

$$\frac{\partial \hat{B}_\theta}{\partial \hat{r}} + \frac{\hat{B}_\theta}{\hat{r}} = \mathcal{E} \hat{T}^{3/2}. \tag{39}$$

Note that $\mathcal{E}(\hat{t})$ can be adjusted by adjusting the rate at which the current in the central solenoid is ramped.

G.   Rescaling

Suppose that the instantaneous minor radius of the plasma is $\delta(\hat{t}) a$. In other words, suppose that the limiter is situated at $\hat{r} = \delta$. Let $x = \hat{r}/\delta$, and let

$$\hat{T}(\hat{r}, \hat{t}) = \frac{\lambda^2}{(\delta \mathcal{E})^4} \bar{T}(x). \tag{40}$$

Equation (38) transforms to give

$$\frac{d^2 \bar{T}}{dx^2} + \frac{1}{x} \frac{d\bar{T}}{dx} + \frac{d \ln \hat{\chi}}{dx} \frac{d\bar{T}}{dx} + \frac{\lambda \bar{T}^{3/2}}{\hat{\chi}} = 0. \tag{41}$$

Appropriate boundary conditions are

$$\bar{T}(0) = 1, \tag{42}$$

$$\frac{d\bar{T}(0)}{dx} = 0, \tag{43}$$

$$\bar{T}(1) = 0. \tag{44}$$

The parameter λ must be adjusted until Eq. (44) is satisfied. Clearly, the determination of the normalized electron temperature profile, $\bar{T}(x)$, involves the solution of a nonlinear eigenvalue problem, where λ is the eigenvalue. Of course, the electron temperature is not zero at the plasma boundary, but is, instead, determined by sheath physics at the plasma/limiter interface. However, we expect the edge temperature to be much lower than that in the plasma interior, which justifies the approximation $\bar{T}(1) = 0$.

10

Let

$$\hat{B}_\theta(\hat{r},\hat{t}) = \frac{\lambda^3}{(\delta\,\mathcal{E})^5}\,\bar{B}_\theta(x). \tag{45}$$

Equation (39) yields

$$\frac{d\bar{B}_\theta}{dx} + \frac{\bar{B}_\theta}{x} = \bar{T}^{3/2}, \tag{46}$$

which must be solved subject to the boundary condition

$$\frac{d\bar{B}(0)}{dx} = 0. \tag{47}$$

Let

$$q(\hat{r},\hat{t}) = \frac{q_a\,\delta\,(\delta\,\mathcal{E})^5}{\lambda^3}\,\bar{q}(x). \tag{48}$$

Equation (28) gives

$$\bar{q}(x) = \frac{x}{\bar{B}_\theta(x)}. \tag{49}$$

Note that

$$\bar{q}(0) = 2. \tag{50}$$

According to Eq. (29), the net normalized toroidal current flowing in the plasma is

$$\hat{I}_p(\hat{t}) = \frac{\lambda^3\,\delta}{(\delta\,\mathcal{E})^5}\,\bar{B}_\theta(1). \tag{51}$$

Equation (36) implies that the normalized ohmic heating power is

$$\hat{P}(\hat{t}) = \frac{\lambda^2}{(\delta\,\mathcal{E})^4}\,\zeta, \tag{52}$$

where

$$\zeta = -\left(\hat{\chi}\,x\,\frac{d\bar{T}}{dx}\right)_{x=1}. \tag{53}$$

According to Eq. (30), the total normalized poloidal magnetic flux contained between the magnetic axis and the plasma boundary is

$$\hat{\psi}_{\text{tot}}(\hat{t}) = \frac{\lambda^3\,\delta}{(\delta\,\mathcal{E})^5}\int_0^1 \bar{B}_\theta\,dx. \tag{54}$$

Finally, the criterion (37) becomes

$$\mathcal{E} > \delta\left|\frac{d}{d\hat{t}}\left[\frac{\lambda^3}{(\delta\,\mathcal{E})^5}\right]\right|\int_0^1 \bar{B}(x)\,dx. \tag{55}$$

Note that we have imposed the criterion at $r = \delta\,a$, rather than $r = a$, because it only needs to be satisfied within the plasma.

IV. CURRENT RAMP SCENARIOS

A. Ramp-Up

1. Introduction

Suppose that the current ramp-up lasts from $t = 0$ to $t = t_{\text{ramp}}$. Suppose that, during the ramp-up, the current in the central solenoid is adjusted such that the normalized plasma current increases linearly in time:

$$\hat{I}_p(\hat{t}) = \frac{\hat{t}}{\hat{t}_{\text{ramp}}}, \tag{56}$$

where $\hat{t}_{\text{ramp}} = t_{\text{ramp}}/\tau_R$.

2. Initial Stage

Suppose that, in the initial stage of the ramp-up, which lasts from $t = 0$ to $t = t_{\text{pre}}$, where $t_{\text{pre}} \ll t_{\text{ramp}}$, the safety-factor at the plasma boundary is allowed to decrease from an initial very large value to its final value, q_a, in such a manner that

$$q(x, \hat{t}) = q_a \left(\frac{\hat{t}_{\text{pre}}}{\hat{t}} \right) \bar{q}(x), \tag{57}$$

where $\hat{t}_{\text{pre}} = t_{\text{pre}}/\tau_R$. Here, q_a is chosen such that $q(0) = 1$ at the end of the initial stage. We make this choice because the sawtooth oscillation effectively prevents the central safety-factor from falling significantly below unity.[17] It follows that

$$q_a = \frac{1}{2 \bar{B}_\theta(1)}. \tag{58}$$

Equations (56) and (57) allow us to determine all other quantities in the initial stage of the ramp-up. We get

$$\delta = \left(\frac{\hat{t}_{\text{pre}}}{\hat{t}_{\text{ramp}}} \right)^{1/2}, \tag{59}$$

which implies that the plasma minor radius takes a relatively small constant value during the first stage of the ramp-up. Furthermore,

$$\hat{T}(x, \hat{t}) = T_{\text{ramp}} \left(\frac{\hat{t}_{\text{pre}}}{\hat{t}_{\text{ramp}}} \right)^{2/5} \left(\frac{\hat{t}}{\hat{t}_{\text{pre}}} \right)^{4/5} \bar{T}(x), \tag{60}$$

$$\hat{B}_\theta(x, \hat{t}) = \left(\frac{\hat{t}_{\text{pre}}}{\hat{t}_{\text{ramp}}}\right)^{1/2} \left(\frac{\hat{t}}{\hat{t}_{\text{pre}}}\right) \frac{\bar{B}_\theta(x)}{\bar{B}_\theta(1)}, \tag{61}$$

$$\mathcal{E}(\hat{t}) = \mathcal{E}_{\text{ramp}} \left(\frac{\hat{t}_{\text{pre}}}{\hat{t}_{\text{ramp}}}\right)^{-3/5} \left(\frac{\hat{t}}{\hat{t}_{\text{pre}}}\right)^{-1/5}, \tag{62}$$

$$\hat{P}(\hat{t}) = P_{\text{ramp}} \left(\frac{\hat{t}_{\text{pre}}}{\hat{t}_{\text{ramp}}}\right)^{2/5} \left(\frac{\hat{t}}{\hat{t}_{\text{pre}}}\right)^{4/5}, \tag{63}$$

$$\hat{\psi}_{\text{tot}}(\hat{t}) = \left(\frac{\hat{t}}{\hat{t}_{\text{ramp}}}\right) \int_0^1 \frac{\bar{B}_\theta(x)}{\bar{B}_\theta(1)} \, dx, \tag{64}$$

where

$$T_{\text{ramp}} = \lambda^{-2/5} \left[\bar{B}_\theta(1)\right]^{-4/5}, \tag{65}$$

$$\mathcal{E}_{\text{ramp}} = \lambda^{3/5} \left[\bar{B}_\theta(1)\right]^{1/5}, \tag{66}$$

$$P_{\text{ramp}} = \zeta \, T_{\text{ramp}}. \tag{67}$$

Finally, the criterion (55) yields

$$\hat{t}_{\text{ramp}} > \left(\frac{\hat{t}_{\text{pre}}}{\hat{t}_{\text{ramp}}}\right)^{3/5} \left(\frac{\hat{t}}{\hat{t}_{\text{pre}}}\right)^{1/5} \mathcal{E}_{\text{ramp}}^{-1} \int_0^1 \frac{\bar{B}_\theta(x)}{\bar{B}_\theta(1)} \, dx, \tag{68}$$

which does indeed constitute a limitation on the maximum current ramp rate.

ACKNOWLEDGEMENTS

DATA AVAILABILITY STATEMENT

The digital data used in the figures in this paper can be obtained from the author upon reasonable request.

---

[1] A.H. Boozer, arXiv preprint arXiv:2507.05456 (2025).

[2] P.C. de Vries, T.C. Luce, Y.S. Bae, S. Gerhardt, X. Gong, Y. Gribov, D. Humphreys, A. Kavin, R.R. Khayrutdinov, C. Kessel, et al., Nucl. Fusion **58** 026019 (2018).

[3] A.H. Boozer, Nucl. Fusion **61**, 054004 (2021).

[4] A.J. Creely, M.J. Greenwald, S.B. Ballinger, D. Brunner, J. Canik, J. Dooly, T. Fülop, D.T. Garnier, R. Granetz, et al., J. Plasma Phys. **86**, 865860502 (2020).

[5] T. Casper, Y. Gribov, A. Kavin, V. Lukash, R. Khayrutdinov, H. Fujieda and C. Kessel, Nucl. Fusion **54**, 013005 (2014).

[6] S.H. Kim, R.H. Bulmer, D.J. Campbell, T.A. Casper, L.L. LoDestro, W.H. Meyer, L.D. Pearlstein and J.A. Snipes, Nucl. Fusion **56**, 126002 (2016).

[7] S.C. Jardin, N. Pomphrey and J. Delucia, J. Comput. Phys. **66**, 481 (1986).

[8] J.B. Lister, A. Portone and Y. Gribov, IEEE Control Systems Magazine **26**, no. 2, 79 (2006).

[9] G. Federici, O. Zolotukhin, M. Kobayashi, A. Loarte, G. Strohmayer, A. Tanga, A. Portone, L. Horton, Y. Feng, F. Sardei, et al., J. Nucl. Materials **363**, 346 (2007).

[10] G.L. Jackson, P.A. Politzer, D.A. Humphreys, T.A. Casper, A.W. Hyatt, J.A. Leuer, J. Lohr, T.C. Luce, M.A. Van Zeeland and J.H. Yu, Phys. Plasmas **17**, 056116 (2010).

[11] P.A. Politzer, G.L. Jackson, D.A. Humphreys, T.C. Luce, A.W. Hyatt and J.A. Leuer, Nucl. Fusion **50**, 035011 (2010).

[12] J.A. Wesson, Nucl. Fusion **18**, 87 (1987).

[13] C.Z. Cheng, H.P. Furth and A.H. Boozer, Plasma Phys. Control. Fusion **29**, 351 (1987).

[14] L. Spitzer, Jr., *Physics of Fully Ionized Gases* (Interscience, New York NY, 1956).

[15] R. Fitzpatrick, *Plasma Physics: An Introduction*, 2nd ed. (CRC, Boca Raton FL, 2023).

[16] R. Fitzpatrick, *Tearing Mode Dynamics in Tokamak Plasmas* (IOP, Bristol UK, 2023).

[17] J.A. Wesson, *Tokamaks*, 4th ed. (Oxford, Oxford UK, 2011).

[18] J.W. Connor and R.J. Hastie, Nucl. Fusion **15**, 415 (1975).

[19] H. Dreicer, Phys. Rev. **115**, 238 (1959).

[20] P.C. de Vries, Y. Gribov, J.R. Martin-Solis, A.B. Mineev, J. Sinha, A.C.C. Sips, V. Kiptily, A. Loarte and JET Contributors, Plasma Phys. Control. Fusion **62**, 125014 (2020).

[21] R. Granetz, B. Eposito, J.H. Kim, R. Koslowski, M. Lehnen, J.R. Martin-Solis, C. Paz-Solden, T. Rhee, J.C. Wesley and L. Zheng, Phys. Plasmas **21**, 072506 (2014).

[22] C. Paz-Solden, N.W. Eidietis, R. Granetz, E.M. Hollmann, R.A. Moyer, J.C. Wesley, J. Zhang, M.E. Austin, N.A. Crocker, A. Wingen and Y. Zhu, Phys. Plasmas **21**, 022514 (2014).

[23] Z. Popovic, B. Esposito, J.R. Martin-Solis, W. Bin, P. Buratti, D. Carnevale, F. Causa, M. Gospodarczyk, D. Marocco, G. Ramogida and M. Riva, Phys. Plasmas **23**, 122501 (2016).
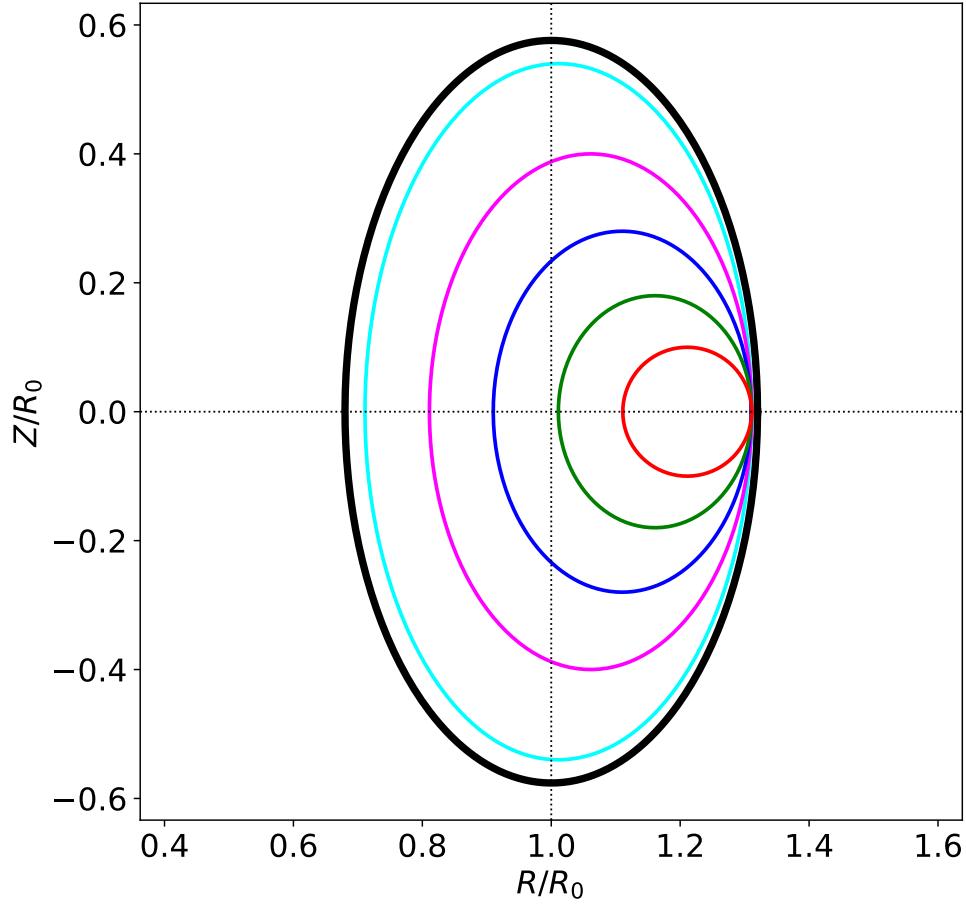
FIG. 1. A cartoon showing the poloidal cross-section of a conventional tokamak during a current ramp-up. The black curve represents the first wall. The red, green, blue, magenta, and cyan curves show, in order of increasing time, the plasma boundary at various stages of the current ramp. Here, R, ϕ, Z are conventional cylindrical coordinates that are co-axial with the plasma torus.